

## MICROBUNCHING PLASMA-CASCADE INSTABILITY\*

V.N. Litvinenko<sup>1,2†</sup>, G. Wang<sup>2,1</sup>, Y. Jing<sup>2,1</sup>, D. Kayran<sup>2,1</sup>, J. Ma<sup>2</sup>, I. Petrushina<sup>1</sup>, I. Pinayev<sup>2</sup>, K. Shih<sup>1</sup>,  
T. Miller<sup>2</sup>, T. Hayes<sup>2</sup>, G. Narayan<sup>2</sup> and Freddy Severino<sup>2</sup>

<sup>1</sup> Department of Physics and Astronomy, Stony Brook University, Stony Brook, NY

<sup>2</sup> Collider-Accelerator Department, Brookhaven National Laboratory, Upton, NY

### Abstract

In this paper we describe a new micro-bunching instability occurring in charged particle beams propagating along a straight trajectory: based on the dynamics we named it a Plasma-Cascade Instability. Such instability can strongly intensify longitudinal micro-bunching originating from the beam's shot noise, and even saturate it. Conversely, such instability can drive novel high-power sources of broadband radiation or can be used as a broadband amplifier. In this paper we present our analytical and numerical studies of this new phenomenon as well as the results of its experimental demonstration.

### PLASMA-CASCADE INSTABILITY

High brightness intense charged particle beams play critical role in the exploration of modern science frontiers [1]. Such beams are central for high luminosity hadron colliders as well as for X-ray femtosecond free-electron-lasers (FEL). In the future, such beams could be central for cooling hadron beams in high-luminosity colliders, X-ray FEL oscillators, and plasma-wake-field accelerators with TV/m accelerating gradients. Dynamics of high intensity beams is driven by both external factors—such as focusing and accelerating fields—and self-induced (collective) effects: space charge, wakefields from the surrounding environment and radiation of the beam. While external factors are designed to preserve beam quality, the collective effects can produce an instability severely degrading beam emittance(s), momentum spread and creating filamentation of the beam. On the other hand, such instabilities can be deliberately built-in to attain specific results such as the FEL instability, Coherent electron Cooling (CeC) or generation of broad-band high power radiation.

The Plasma-Cascade micro-bunching Instability (PCI) occurs in a beam propagating along a straight line. It is driven by variation of the transverse beam size(s) [1]. Conventional micro-bunching instability for beams travelling along a curved trajectory is a well-known and in-depth studied both theoretically and experimentally [2-20]. Space-charge-driven parametric transverse instabilities are also well known (see review [21] and references therein). But none of them include the PCI—a micro-bunching longitudinal instability driven by modulations of the transverse beam size. Figure 1 depicts a periodic focusing structure where the charged particle beam undergoes periodic variations of its transverse size.

It is known that small density perturbations  $\tilde{n}(\vec{r}), |\tilde{n}| \ll n_o$  in a cold, infinite and homogeneous charged beam will undergo oscillations with plasma frequency,  $\omega_p = c\sqrt{4\pi n_o r_c}$  [22], where  $n_o$  is the particles density (in beam's co-moving frame),  $c$  is the speed of light and  $r_c = e^2 / mc^2$  is particle's classical radius.

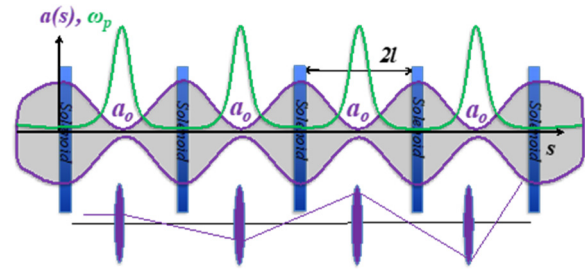


Figure 1: A sketch of four focusing cells with periodic modulations of beam envelope,  $a(s)$ , and the plasma frequency,  $\omega_p$ . Beam envelope has waists,  $a_o$ , in the middle of each cell where plasma frequency peaks. Scales are attuned for illustration purpose. The bottom sketch illustrates an unstable ray trajectory in a system of periodic focusing lenses—an analogue of unstable longitudinal oscillations. The waists of the beam serve as “short focusing elements” for the longitudinal plasma oscillations.

Beam propagating with velocity  $v_o$  through the lattice (with period  $2l$ ) would experience density modulation in the co-moving frame with period of  $T = 2l / \gamma_o v_o$ :

$$f_{\perp} = n_o(t) = \frac{I_o}{e\beta_o \gamma_o c \pi a^2 (\gamma_o \beta_o ct)} \quad (1)$$

where  $I_o$  is the beam current and  $\gamma_o = (1 - \beta_o^2)^{-1/2}$ ,  $\beta_o = v_o / c$  is the beam's relativistic factor.

It is well known [23] that modulation of oscillator frequency with a period close twice of oscillation period would result in exponential growth of oscillation amplitude: the phenomena known as parametric resonance. The extreme case of  $\delta$ -function-like modulation is well known: periodic focusing lenses with focal length shorter than a quarter of the separating distances will make rays unstable and the entire half-space  $F < l/2$  is occupied by this parametric resonance.

### ANALYTICAL STUDIES

In mathematical terms, we need to separate transverse and longitudinal degrees of freedom:  $f = f_{\perp} \cdot f_{\parallel}$ . For

\* Work is supported by Brookhaven Science Associates, LLC under Contract No. DEAC0298CH10886 with the U.S. Department of Energy, DOE NP office grant DE-FOA-0000632, and NSF grant PHY-1415252.

† vladimir.litvinenko@stonybrook.edu

compactness, we will consider only case of periodic axially-symmetric systems with round beams. Following [1] we considered a long bunch  $\sigma_s \gg a / \gamma_o$  with transverse Kapchinsky-Vladimirsky (KV) distribution [24] providing uniform density inside the beam envelope,  $r \leq a(s)$ , and zero density outside it [25]. Detailed theoretical derivation can be found in [1,26] where we followed methods developed in [26-29] for  $\kappa$ -1 longitudinal velocity distribution  $f_o(v) = \sigma_v / \pi(\sigma_v^2 + v^2)$  and the beam envelope differential equation [25] to derive a set of dimensionless equations for periodic systems:

$$\frac{d^2 \hat{a}}{d\hat{s}^2} - k_{sc}^2 \hat{a}^{-1} - k_\beta^2 \hat{a}^{-3} = 0; \quad \frac{d^2 \tilde{n}_k}{d\hat{s}^2} + 2 \frac{k_{sc}^2}{\hat{a}(\hat{s})^2} \cdot \tilde{n}_k = 0; \quad (2)$$

$$\hat{a} = \frac{a}{a_o}; \quad \hat{s} = \frac{s}{l}; \quad k_{sc} = \sqrt{\frac{2}{\beta_o^3 \gamma_o^3} \frac{I_o}{I_A} \frac{l^2}{a_o^2}}; \quad k_\beta = \frac{\epsilon l}{a_o^2}.$$

where  $\epsilon$  is the envelope emittance,  $I_A = mc^3 / e \approx 17 \text{ kA}$  is the Alfvén current,  $\tilde{n}_k$  is longitudinal density perturbation corrected by Landau damping  $\exp(k\sigma_v t)$  [30-31] and with variables  $\hat{a} \geq 1; \hat{s} \in \{-1, 1\}$

$$\frac{d^2 \hat{a}}{d\hat{s}^2} - k_{sc}^2 \hat{a}^{-1} - k_\beta^2 \hat{a}^{-3} = 0; \quad \frac{d^2 \tilde{n}_k}{d\hat{s}^2} + 2 \frac{k_{sc}^2}{\hat{a}(\hat{s})^2} \cdot \tilde{n}_k = 0; \quad (7)$$

$$\hat{a} = \frac{a}{a_o}; \quad \hat{s} = \frac{s}{l}; \quad k_{sc} = \sqrt{\frac{2}{\beta_o^3 \gamma_o^3} \frac{I_o}{I_A} \frac{l^2}{a_o^2}}; \quad k_\beta = \frac{\epsilon l}{a_o^2}.$$

with variables  $\hat{a} \geq 1; \hat{s} \in \{-1, 1\}$ . The system dynamics defined by two parameters representing space charge and emittance effects:  $k_{sc}$  and  $k_\beta$ . Figure 2 shows the growth rate per cell in such system [32] evaluated by a semi-analytical code in Mathematica [33] using 4-th order symplectic integrators [34]. The growth rates peak along the ridge  $k_\beta = 3 \cdot (k_{sc} - 1.2)$  and can be estimated there as  $\lambda \propto 1.25 k_{sc} \approx 1.5 + 0.413 k_\beta$ .

## NUMERICAL STUDIES

While both qualitative and semi-analytical studies reveal the nature of the PCI, modern particle-in-cell codes allow 3D investigations of PCI without any predetermined assumptions. We used code SPACE [35-36] for accurate simulation of PCI in electron beam with constant beam energy propagating along the straight section with focusing solenoids. Using this code, we confirmed that indeed the PCI could occur in periodic and aperiodic beamlines for a wide range of parameters, modulation frequencies and beam energies. Three sets of parameters listed in Table 1 were used in our studies. Figure 3 shows simulation results for two test cases of the periodic lattices with PCI at 25 THz and 1 PHz (1,000 THz). Case of the aperiodic lattice is related to our experiment and is described in the next section and illustrated in Figs. 4 and 5.

Each cell consists of a drift section with a length of  $2l$  between the two focusing solenoids. Initial conditions for this simulation included shot noise and a weak longitudinal density modulation. The beam envelope at the entrance and solenoid strengths are selected to provide the designed beam envelope with waists  $a_o$  in the middle of each cell. Amplitude of density modulation,  $\tilde{g}_k$ , is tracked as a function of the propagation distance. The 3D simulations confirmed our expectations that PCI, as shown in clip in Fig. 3, is a broad-band instability

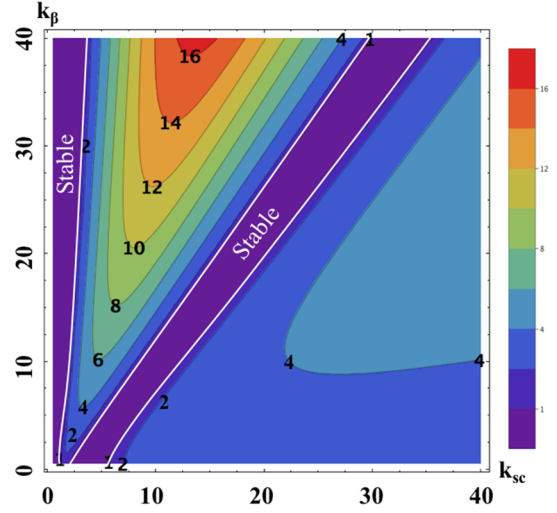


Figure 2: Contour plots of  $\lambda = \max(|\text{Re } \lambda_1|, |\text{Re } \lambda_2|)$ , absolute value of the growth rate per cell. Purple area highlighted by white lines  $|\lambda_{1,2}| = 1$  is areas of stable oscillations.

Table 1: Beam Parameters for PCI Simulations and Tests

Name	Exp	Case 1	Case 2
Lattice	Aperiodic	Periodic	Periodic
	LEBT	4 cells	4 cells
$\gamma$	3.443	28.5	275
<b>E, MeV</b>	<b>1.76</b>	<b>14.56</b>	<b>140.5</b>
$l, m$	1.5 - 3	1	10
$a_o, mm$	0.3, min	0.2	0.1
$I_o, A$	1.75	100	250
$\epsilon_{norm}, m$	$1 \cdot 10^{-6}$	$8 \cdot 10^{-6}$	$4 \cdot 10^{-4}$
$k_{sc}$	Varies	3.56	3.76
$k_\beta$	Varies	7.02	14.55
$\lambda_1, \text{ per cell}$	N/A	-4.06	-5.10
Energy spread	$1 \cdot 10^{-4}$	$1 \cdot 10^{-4}$	$1 \cdot 10^{-4}$
Frequency, THz	<b>0.4</b>	<b>25</b>	<b>1,000</b>

## EXPERIMENTAL DEMONSTRATION

We experimentally observed broad-band PCI at frequencies  $\sim 0.5 \text{ THz}$  and  $\sim 10 \text{ THz}$  using linear superconducting (SRF) accelerator, shown in Fig. 4, built for the CeC experiment. We used 400 psec electron bunches with

Content from this work may be used under the terms of the CC BY 3.0 licence (© 2019). Any distribution of this work must maintain attribution to the author(s), title of the work, publisher, and DOI

various charges generated in the 1.25 MV SRF photocathode gun. Two room temperature RF 500 MHz cavities were used to correct the gun's RF curvature and reduce energy spread in the bunch to 0.01% level. Strong-focusing aperiodic lattice comprised of six solenoids in the low energy beam transport (LEBT) and provided beam envelope shown in Fig.4. To observe the density modulation in the beam we transformed our linac and dipole beam-line into a time-resolving system with sub-psec resolution. We operated the linac at zero crossing with low accelerating voltage,  $V \sim 100\text{-}200$  kV, to correlate particle's energy with the arriving time  $E = E_0 + eV \sin \omega_L t$ . The 45° dipole and the profile monitor 4 served as the energy spectrometer. The measured energy distribution was a carbon copy of the bunch's time profile.

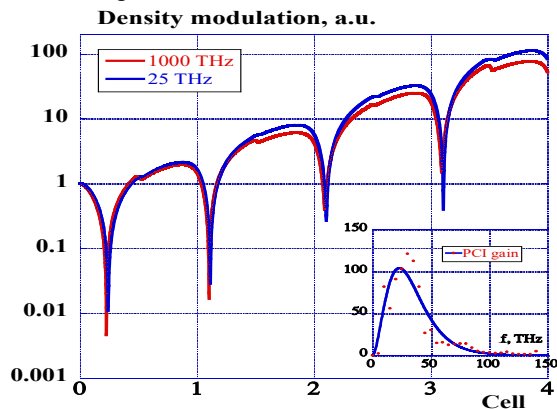


Figure 3: Evolution of density modulation amplitude in 4-cell PCI periodic lattice with parameters shown in Table 1: Blue line, Case 1, gain = 114; Red line, Case 2, gain=75. The PCI gain spectrum for Case 1 is shown in a clip in the bottom-right corner: red dots are FFT of the amplified shot noise and the blue curve is a smooth fit.

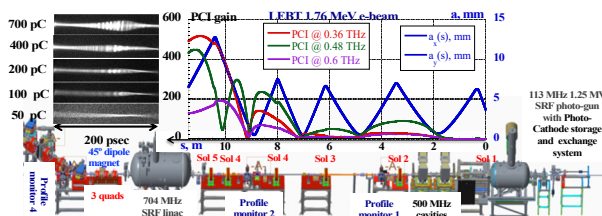


Figure 4: Layout of the CeC accelerator (right to left): the SRF electron gun, two bunching RF cavities, the LEBT line equipped with six solenoids and two profile monitors, followed by the 13.1 MeV SRF linac and a 45° bending magnet beam line (with three quadrupoles and a beam profile monitor). The top graph shows simulated (by code SPACE) evolutions in the LEBT of the beam envelope  $a(s)$ , blue line and PCI gains at frequencies of 0.36 THz (red line), 0.48 THz (violet), and 0.6 THz (green). Simulations were done for 1.75 MeV ( $\gamma=3.443$ ), 0.7 nC, 0.4 nsec electron bunch with 1  $\mu\text{m}$  normalized slice emittance and 0.01% slice RMS energy spread. Clip in the left-top corner shows time-resolved bunch profiles.

Time resolution of our measurement system depends on the linac voltage. We found that the best data quality

was obtained at 100 kV setting with resolution of 7 pixel/psec at the digital camera. Figure 5 shows a few selected density profiles measured by our system as well as their spectra.

We observed a very large,  $\pm 50\%$ , density modulation that can be seen both in the captured images, or in the density profiles in Fig.5 (a) and (c). Figure 5 (b) shows measured bunch spectra, which compares very well with the simulation: a broadband PCI gain peaking at  $\sim 0.4$  THz. The high and low frequency noise floor is determined by the noise in the CCD camera and it is  $\sim 100$  higher than natural shot noise in the beam. The calculated correlation length of the density modulation  $\sim 1.5$  and large spectral bandwidth of instability  $\Delta f/f \sim 1$  are in good agreement.

While all our measurements were in good agreement with our simulations, to clarify that the observed structures were indeed caused by the PCI we performed simulations of beam dynamics including and excluding wakefields from the beam-line components in LEBT (calculated using codes CST [37], Echo [38], and ABCI ) and found no signatures at frequencies above 0.1 THz.

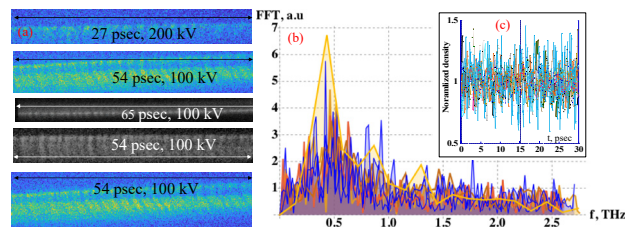


Figure 5: (a) Measured time profiles of 1.75 MeV electron bunches emerging from LEBT. Charge per bunch was from 0.45 nC to 0.7 nC; (b) Seven overlapping spectra of measured bunch density modulation and PCI spectrum simulated by SPACE (slightly elevated yellow line); (c) Clip shows a 30-psec fragment of seven measured relative density modulations.

Nominally, for CeC operations, we compress electron bunches 20-fold in LEBT by applying energy chirp. This provided us with an opportunity to observe PCI at frequencies  $\sim 10\text{THz}$ . Simulations using Impact-T code [39] clearly indicated broad-band PCI with gain  $\sim 15\text{-}20$  at and around frequency of 10 THz. We used broad-band IR diagnostic to measure radiation power from our 45-degree bending magnet and found that it exceeded level of natural (e.g. originated from Poisson statistics) spontaneous radiation  $\sim 300 \pm 100$  fold, again is in reasonable agreement with the predicted increase in the amplitude of the density modulation  $\sim 15\text{-}20$ -fold.

## CONCLUSION

In conclusion, we would like to announce the discovery of a novel microbunching instability occurring in charged particle beams propagating along a straight trajectory—Plasma-Cascade Instability.

## REFERENCES

[1] V.N. Litvinenko, G. Wang, D. Kayran, Y. Jing, J. Ma, I. Pinayev, arXiv:1802.08677, 2018.

- Any distribution of this work must maintain attribution to the author(s), title of the work, publisher, and DOI (© 2019).
- CC BY 3.0 licence
- Content from this work may be used under the terms of the
- [2] A. Chao, E. Granados, X. Huang, D. F. Ratner and H. W. Luo, “High Power Radiation Sources using the Steady-state Microbunching Mechanism”, in *Proc. 7th Int. Particle Accelerator Conf. (IPAC'16)*, Busan, Korea, May 2016, pp. 1048-1053. doi:10.18429/JACoW-IPAC2016-TUXB01
- [3] D.F. Ratner, A.W.Chao, *Phys. Rev. Lett.* **28**,154801, 2010.
- [4] Y. Jiao, D.F. Ratner, A.W. Chao, *Phys. Rev. ST Accel. Beams* **14**, 33702, 2011.
- [5] R.A. Lacey, *Phys. Rev. Lett.* **114**, 142301, 2015.
- [6] E. L. Saldin, E. A. Schneidmiller and M.V. Yurkov, *NIM A* **490**, 1, 2002.
- [7] S. Heifets, G. Stupakov and S. Krinsky, *Phys. Rev. ST Accel. Beams* **5**, 064401, 2002.
- [8] E. A. Schneidmiller and M.V. Yurkov, *Phys. Rev. ST Accel. Beams* **13**, 110701, 2010.
- [9] T. Shaftan and Z. Huang, *Phys. Rev. ST-AB*, **7**:080702, 2004.
- [10] Marco Venturini, *Phys. Rev. ST Accel. Beams*, **10**, 104401, 2007.
- [11] M. Venturini, *Phys. Rev. ST Accel. Beams*, **11**:034401, 2008.
- [12] D. F. Ratner, A. Chao, and Z. Huang, “Three-dimensional Analysis of Longitudinal Space Charge Microbunching Starting from Shot Noise”, in *Proc. 30th Int. Free Electron Laser Conf. (FEL'08)*, Gyeongju, Korea, Aug. 2008, paper TUPPH041, pp. 338-341.
- [13] R. Akre *et al.*, *Phys. Rev. ST Accel. Beams*, **11**, 030703, 2008.
- [14] A. Marinelli and J.B. Rosenzweig, *Phys. Rev. ST Accel. Beams* **13**, 110703, 2010.
- [15] A. Marinelli *et al.*, *Phys. Rev. Lett.* **110**, 264802 (2013).
- [16] Z. Huang and K-J. Kim, *Phys. Rev. ST Accel. Beams* **5**, 074401, 2002.
- [17] Z. Huang *et al.*, *Phys. Rev. ST Accel. Beams* **7**, 074401, 2004.
- [18] D. Ratner, PhD thesis, Department of Applied Physics, Stanford University, 2011.
- [19] A. Marinelli, E. Hemsing, and J.B. Rosenzweig, *Physics of Plasmas*, **18**:26105, 2011.
- [20] D. Ratner, *ICFA Beam Dynamics Newsletter* No. 49 p. 35, 2012.
- [21] A. Fedotov *et al.*, *PR STAB* **6**, 094201, 2003
- [22] D.R. Nicholson, Introduction in Plasma Theory, John Wiley & Sons, 1983.
- [23] L.D. Landau, E.M. Lifshitz, Classical Mechanics.
- [24] I.M. Kapchinsky and V.V. Vladimirovsky, *Proc. Int. Conf. on High-Energy Accelerators and Instrumentation*, CERN, 1959, p. 274.
- [25] M. Reiser, Theory and design of charged particle beams, John Wiley & Sons, 2008.
- [26] V. N. Litvinenko *et al.*, arXiv:1902.10846, 2019.
- [27] G.Wang, PhD Thesis, 2008, State University of New York at Stony Brook.
- [28] G.Wang, M.Blaskiewicz, *Phys Rev E*, volume 78, 026413, 2008.
- [29] G. Wang, M. Blaskiewicz, and V. Litvinenko, “Simulation of Ion Beam under Coherent Electron Cooling”, in *Proc. 7th Int. Particle Accelerator Conf. (IPAC'16)*, Busan, Korea, May 2016, pp. 1243-1246. doi:10.18429/JACoW-IPAC2016-TUPMR008
- [30] L.D. Landau, *JETP* **16** (1946), 574.
- [31] Collected papers of L.D. Landau, Pergamon Press, 1965, p. 445.
- [32] E.D. Courant, H.S. Snyder, *Ann. Phys.* **3** (1958) 1.
- [33] Wolfram Research, Inc., Mathematica.
- [34] E. Forest, “Forth-order symplectic integrator”, SLAG-PUB-5071, LBL-27662, August 1989.
- [35] X. Wang, R. Samulyak, J. Jiao, K. Yu, *J. Comput. Phys.*, **316**, pp. 682 – 699, 2016.
- [36] K. Yu and V. Samulyak, “SPACE Code for Beam-Plasma Interaction”, in *Proc. 6th Int. Particle Accelerator Conf. (IPAC'15)*, Richmond, VA, USA, May 2015, pp. 728-730. doi:10.18429/JACoW-IPAC2015-MOPMNO12
- [37] V. Litvinenko *et al.*, “Commissioning of FEL-Based Coherent Electron Cooling System”, in *Proc. 38th Int. Free Electron Laser Conf. (FEL'17)*, Santa Fe, NM, USA, Aug. 2017, pp. 132-135. doi:10.18429/JACoW-FEL2017-MOP041
- [37] CST—Computer Simulation Technology, 2017.
- [38] I. Zagorodnov, Wakefield Code ECHO, 2016,
- [39] Ji Qiang, IMPACT-T.fa